Synthesis and Optical Properties of Thermotropic Polythiophene and Poly(*p*-phenylene) Derivatives

Shaw H. Chen,*,†,‡,§,∥ Brooke M. Conger,†,‡ John C. Mastrangelo,§ Andrew S. Kende,§,⊥ and Dong U. Kim∥

Materials Science Program, Departments of Chemical Engineering and Chemistry, NSF Center for Photoinduced Charge Transfer, and Laboratory for Laser Energetics, Center for Optoelectronics and Imaging, University of Rochester 240 East River Road, Rochester, New York 14623-1212

Received June 15, 1998; Revised Manuscript Received September 13, 1998

ABSTRACT: Thermotropic nematic and chiral-nematic conjugated polymers consisting of polythiophene and poly(*p*-phenylene) backbones carrying cyanobiphenyl and (−)-cholesterol as pendant groups were synthesized and characterized as a new class of optical polymers. Spontaneous assembly of the conjugated backbone was promoted by liquid crystalline mesomorphism on the part of the pendants, thereby allowing uniaxially and helically aligned glassy films to be prepared for polarized photoluminescence (PL) studies. In the thiophene series, the conjugated backbone was found to yield an absorption peak red-shifted from those of the monomers and pendant groups. This permitted selective photoexcitation of the polythiophene backbone to be accomplished. In the *p*-phenylene series, the conjugated backbone did not give rise to a unique absorption peak. However, with excitation at the long wavelength edge of the absorption peak, PL of the poly(*p*-phenylene) backbone was found to be 1 order of magnitude stronger than that of the pendant cyanobiphenyl group. These ordered solid films produced significant degrees of linearly and circularly polarized PL. Existing theories were found to be capable of representing the experimental results with independently measured absorption coefficient, average refractive index, and optical birefringence.

I. Introduction

Uniaxial, lamellar, helical, and columnar molecular arrangements on a macroscopic scale can be realized through liquid crystal formation as molecular self-organization. If these molecular arrangements could be frozen into the solid state, the resultant "liquid crystalline glass" would be ideally suited for a broad range of optical and electronic applications, such as light polarization[1] and photoconductivity.[2] However, most liquid crystals tend to form polycrystalline films on cooling from the mesomorphic temperature range, causing light scattering or hindering charge carrier mobility. Therefore, there has been a strong motivation for developing liquid crystalline materials that will bypass crystallization on cooling while preserving various molecular orders in the glassy state. One approach takes advantage of glass formation by polymeric systems, such as side-chain liquid crystalline polymers in which pendant groups are responsible for liquid crystallinity. From an entirely different perspective, π-conjugated polymers have been extensively investigated over the last two decades for various electronic and optical applications. Intensive research has been devoted in particular to exploring the potential for use as thin film transistors,[3] light-emitting diodes,[4] and organic lasers.[5] The hybrid system comprising a π-conjugated backbone to which liquid crystalline pendants are chemically bonded represents a new class of multifunctional organic materials potentially capable of enhancing existing, and creating novel, electronic and optical properties. Nematic and smectic conjugated polymers have been explored to enhance conductivity,[6] to produce linearly polarized emission,[7] and to impart new features to electrochromism,[8] all attempting to take advantage of the macroscopic order inherent to liquid crystal mesomorphism.

Polarized light is essential to optical information processing and display. Passive (i.e., nonemitting) devices are available for accomplishing linear and circular polarization based on anisotropic absorption[9] and selective reflection,[10] respectively, of unpolarized incident light. Active (i.e., light-emitting) devices via photo- or electroexcitation represent a technological advance over passive devices. For linearly polarized photoluminescence (LPPL) from uniaxially aligned luminophores, various methodologies have been successfully demonstrated, such as mechanical stretching,[11,12] the Langmuir−Blodgett technique,[13] and nematic mesomorphism.[14] Circularly polarized photoluminescence (CPPL) has been explored with polythiophene twisted with chiral pendants.[15] We have shown that a high degree of circular polarization can be accomplished with a helical arrangement of luminophores mediated by cholesteric mesomorphism.[16] In a recent communication, we have presented the first example of chiral-nematic polythiophene derivatives[17] with an objective of introducing helically oriented π-conjugated systems. This novel class of materials was explored for LPPL and CPPL in the present study.

II. Experimental Section

Synthesis of Monomers and Polymers. The chemical structures of mesomorphic monomers and polymers synthesized for this study are summarized in Figure 1. The synthesis and characterization of the thiophene monomers, I and II, and polymers III-*x*, where *x* denotes the mole fraction of the cholesteryl pendant, are as described in a recent communica-

* To whom correspondence should be addressed.
† Materials Science Program.
‡ Department of Chemical Engineering.
§ NSF Center for Photoinduced Charge Transfer.
∥ Department of Chemistry.
⊥ Laboratory for Laser Energetics.

10.1021/ma980945p CCC: $15.00
Published on Web 10/22/1998

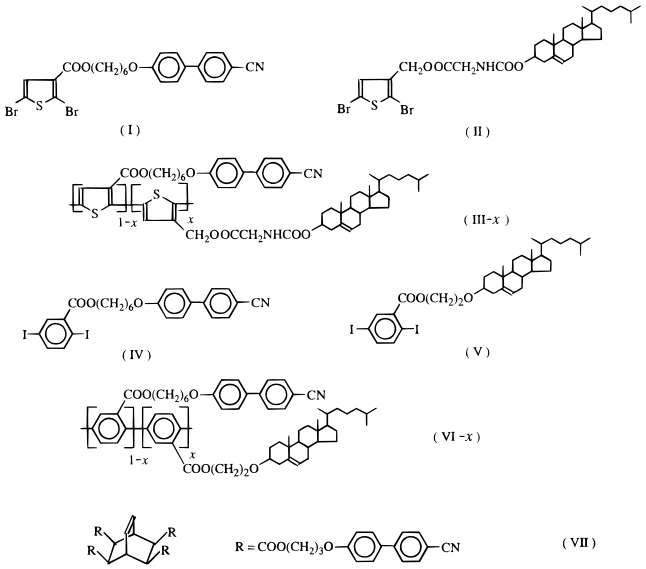

Figure 1. Molecular structures of monomers, polymers, and a glass-forming liquid crystal employed in the present study.

Scheme 1. Synthesis of Monomers IV and V and Polymer VI-*x*

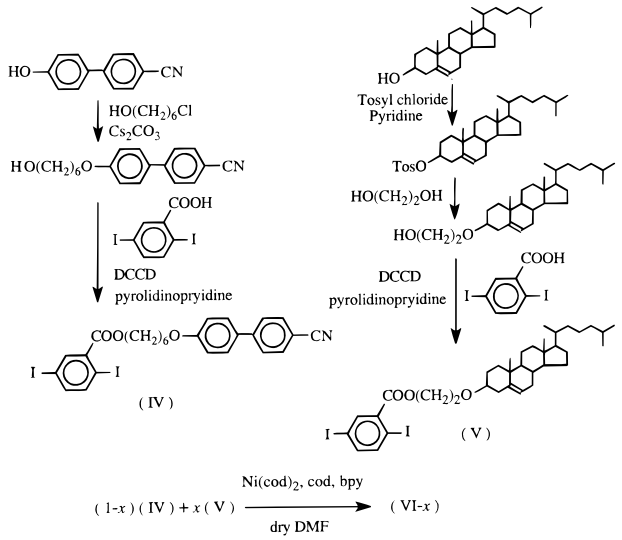

tion.[17] Compound VII, a nematic glass-forming liquid crystal, has also been reported previously.[18] Synthesis of *p*-phenylene monomers and polymers, i.e. IV, V, and VI-*x*, was conducted in accordance with the reaction in Scheme 1 using reagents and chemicals all received from Aldrich Chemical Co.

4-(6-Hydroxyhexyloxy)-4′-cyanobiphenyl. 4-Hydroxy-4′-cyanobiphenyl (20.61 g, 105 mmol), 6-chloro-1-hexanol (17.00 g, 124 mmol), cesium carbonate (37.10 g, 113 mmol), and potassium iodide (0.18 g, 1.1 mmol) were dissolved in 260 mL of DMF. The reaction mixture was stirred at 80 °C for 5 h. The insolubles were removed by hot filtration. The hot filtrate was slowly added to 1.5 L of water, and the solids were filtered. The crude product was purified by recrystallization from methanol to produce 21.97 g in 70% yield.

6-[4-[(4′-Cyanobiphenyl)yl]oxy]hexyl 2,5-diiodobenzoate, (IV). Under a dry nitrogen atmosphere, 8.66 g of 2,5-diiodobenzoic acid (23.2 mmol), 6.63 g of 4-(6-hydroxyhexyloxy)-4′-cyanobiphenyl (22.5 mmol), 0.40 g of 4-pyrolidinopyridine (2.70 mmol), and 6.07 g of *N*,*N*′-dicyclohexylcarbodiimide, DCCD (29.4 mmol) were dissolved in 140 mL of anhydrous THF and stirred for 5 h. The insolubles were filtered off, and the THF was removed by evaporation in vacuo. The residue was shaken with 100 mL of methylene chloride and 100 mL of 10% HOAc(aq). The insolubles were removed by filtration, and the organic layer was dried with anhydrous $MgSO_4$. Methylene chloride was removed by evaporation in vacuo. The crude product was purified by recrystallization from a 50/50 mixture of acetone and methanol to produce (IV) in 86% yield. NMR ($CDCl_3$) spectral data: δ 8.10−7.00 (m, aromatic, 11H), 4.35 (t, COOC**H**$_2$, 2H), 4.10 (t, C**H**$_2$OAr, 2H), 1.90 (d, OCH$_2$C**H**$_2$, 4H), 1.60 (d, (CH$_2$)$_2$C**H**$_2$(CH$_2$)$_2$, 4H). Anal. Calcd for $C_{26}H_{23}O_3NI_2$: C, 47.95; H, 3.56; N, 2.15; I, 38.97. Found: C, 47.55; H, 3.55; N, 2.20; I, 37.83.

Cholesteryl *p*-Toluenesulfonate. Naturally occurring (−)-cholesterol (20 g, 51.7 mmol) was dissolved in 100 mL of anhydrous pyridine under a dry nitrogen atmosphere, to which tosyl chloride (19.72 g, 103 mmol) was added. The mixture was allowed to stir for 16 h before adding 200 mL of water at 0 °C. The solid collected via filtration was washed with 200 mL of water twice. The crude product was purified by recrystallization from acetone to produce 22.01 g in 79% yield.

2-[3*β*-(5-Cholestenyl)oxy]ethanol. Cholesteryl *p*-toluenesulfonate (21.74 g, 40.2 mmol) was dissolved in a mixture of 145 mL of ethylene glycol and 300 mL of dioxane. The reaction mixture was stirred at 80 °C for 2 h. Water (100 mL) was then added to the reactor, and the azeotropic mixture of water and dioxane was removed by evaporation in vacuo. The residue was then shaken with 400 mL of water and 200 mL of diethyl ether. The organic layer was dried with anhydrous $MgSO_4$ before evaporation to dryness. Petroleum ether (100 mL) was added to the solid residue, and the yellow liquid was removed by filtration. The white solid was washed with petroleum ether and then purified by recrystallization from hexanes to produce 12.2 g in 71% yield.

2-[3*β*-(5-Cholestenyl)oxy]ethyl 2,5-Diiodobenzoate (V). The cholesteryl monomer, compound V, was prepared by the same procedures as the cyanobiphenyl monomer, compound IV, except using 2-[3*β*-(5-cholestenyl)oxy] ethanol in place of 4-(6-hydroxyhexyloxy)-4′-cyanobiphenyl. The crude product was purified by recrystallization in a 50/50 mixture of methylene chloride and hexanes to produce V in 72% yield. NMR ($CDCl_3$) spectral data: δ 8.15 (s, aromatic, 1H), 7.70 (d, aromatic, 1H), 7.45 (d, aromatic, 1H), 5.35 (m, **H**C═C, chol, 1H), 4.45 (t, COOC**H**$_2$CH$_2$, 2H), 3.85 (t, OC**H**$_2$CH$_2$, 2H), 3.25 (m, **H**C−O chol, 1H), 2.50−0.60 (m, chol skeleton, 43H). Anal. Calcd for $C_{36}H_{52}O_3I_2$: C, 54.97; H, 6.66; I, 32.27. Found: C, 55.11; H, 6.68; I, 31.55.

Nematic Homopolymer (VI-0.00). Under a dry nitrogen atmosphere, a mixture was prepared for condensation polymerization: monomer IV (1.496 g, 2.3 mmol), 0.32 mL of 1,5-cyclooctadiene (2.6 mmol), 0.90 g of bis(1,5-cyclooctadiene)-nickel(0) (3.3 mmol), and 0.438 g of 2,2′-bipyridyl in 9 mL of anhydrous DMF. The reaction mixture was stirred at 55 °C for 16 h. Subsequently, a mixture of 100 mL of methanol and 2 mL of HCl was added, and the insolubles were filtered off. The filtrate was washed with ethanol, basic EDTA, acidic EDTA, water, and ethanol. Methylene chloride was added (10 mL), and the insolubles were filtered off. The crude product was purified by spray precipitation into acetone to produce 0.33 g in 36% yield. The dissolution−precipitation cycles were repeated till monomer peaks disappeared from the gel permeation chromatograms. NMR ($CDCl_3$) spectral data: δ 8.40−6.80 (m, aromatic, 11H), 4.30−3.60 (m, OC**H**$_2$CH$_2$, 4H), 1.90−1.20 (m, CH$_2$C**H**$_2$CH$_2$, 8H). Anal. Calcd for $(C_{26}H_{23}O_3N)_{17}I_2$: C, 74.55; H, 5.53; N, 3.34; I, 3.56. Found: C, 74.75; H, 5.48; N, 3.44; I, 3.76.

Chiral-Nematic Copolymer (VI-0.07). The chiral nematic copolymer (VI-0.07) was prepared by following the same procedures as for the nematic homopolymer (VI-0.00), except using a 9:1 mixture of monomers IV and V. The crude product was purified by spray precipitation into a 30:1 mixture of methanol and acetone to produce 0.60 g in 60% yield. NMR ($CDCl_3$) spectral data: δ 8.40−6.80 (m, aromatic, x(3H) + (1 − x)(11H)), 5.35 (m, **H**C═C, chol, x(1H)), 4.50−3.80 (m, OC**H**$_2$, x(4H) + (1 − x)(4H)), 3.50 (m, **H**C−O chol, x(1H)), 2.50−0.60 (m, chol skeleton, x(43H) + CH$_2$C**H**$_2$CH$_2$, (1 − x)(8H)); x = 0.07, a value close to the feed composition.

Characterization of Molecular Structures and Thermotropic Properties. Chemical structures were elucidated

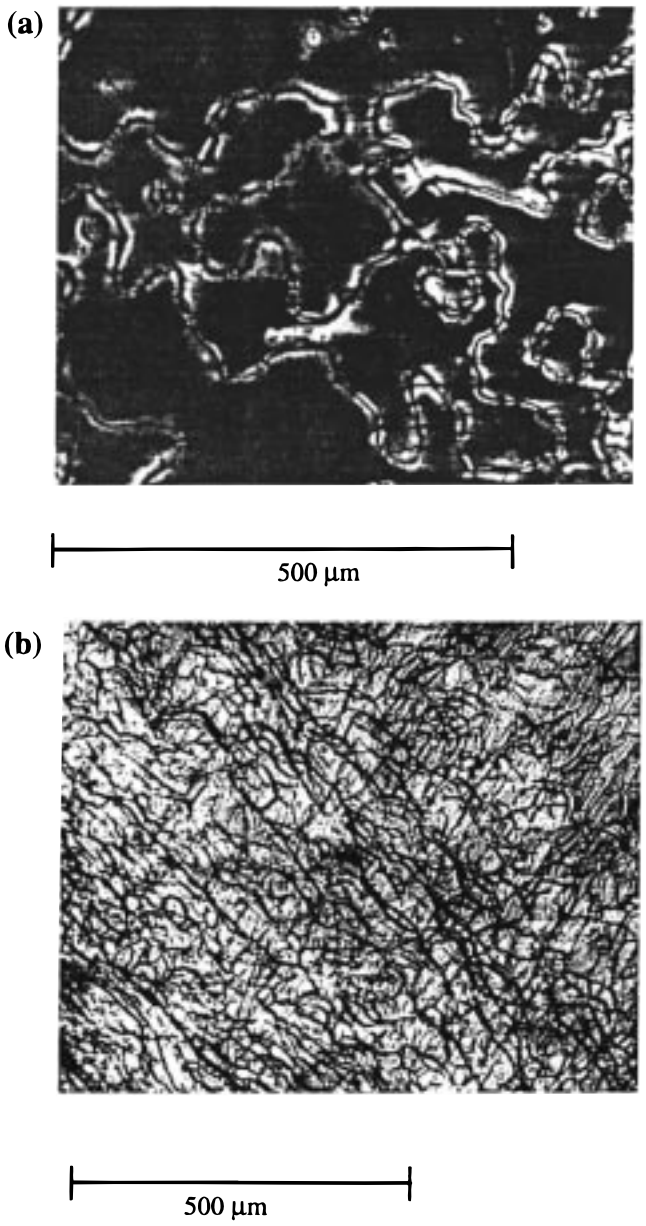

Figure 2. Polarizing optical micrographs: (a) nematic threaded textures of VI-0.00; (b) cholesteric oily streaks of VI-0.07.

with elemental analysis (performed by Oneida Research Services, Inc., Whitesboro, NY), FTIR (Nicolet 20 SXC), and ^{1}H NMR (QE−300, GE) spectroscopic techniques. The chiral mole fraction, x, of copolymers was determined by an integration of relevant ^{1}H NMR signals, and the values were found to be consistent with the feed composition. Thermal transition temperatures were determined by DSC (Perkin-Elmer DSC-7) with a continuous nitrogen purge at 20 mL/min. Liquid crystal mesomorphism was determined with a polarizing optical microscope (Leitz Orthoplan-Pol) equipped with a hot stage (FP82, Mettler) and a central processor (FP80, Mettler). As illustrated in Figure 2, the nematic and cholesteric mesomorphism were identified with the threaded textures and oily streaks, respectively. A gel permeation chromatograph (GPC) was employed to determine the molecular weight distribution with reference to polystyrene standards, from which the number- and weight-average molecular weights, $\bar{M}_n$ and $\bar{M}_w$, were calculated.

Vitrified Thin Film Preparation. For the fabrication of vitrified liquid crystalline films, two fused silica substrates (Escoproducts, 1 in. diameter × $^1/_8$ in. thickness, with n = 1.458) with nylon alignment coating were heated to a temperature of 10−20 °C below the clearing point of the sample.

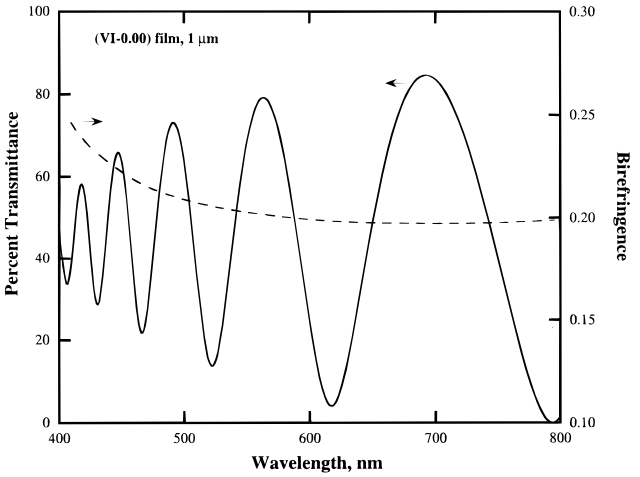

Figure 3. Optical transmittance and birefringence of a 1.0 μm film of VI-0.00.

The optical elements were made by sandwiching the material between the two substrates, using glass sphere or fiber spacers to control the thickness. The top substrate was then pressed and sheared to form a uniform, aligned film. The device was clamped and annealed at 95% of the clearing temperature on an absolute temperature scale. The typical annealing time for conjugated polymers III and VI ranged from 3 days to 1 week, whereas it took 3 h for VII, a glass-forming liquid crystal, to achieve a comparable order parameter. Subsequent cooling at −30 °C/h to room temperature contributed to the formation of macroscopically ordered, solidified thin films. The samples for the refractometric characterization were prepared as above between a low refractive index substrate, calcium fluoride (Optovac, 1 in. diameter × 0.039 in. thickness, with n = 1.4325) substrate, and a high refractive index substrate, SF_6 (n = 1.8046 at 589 nm).

Characterization of Optical Properties. A spectrophotometer (Perkin-Elmer Lambda 9) was employed to determine UV−vis absorption and the thickness of films. The peaks of interference fringes of the air gap between the substrates were used to calculate the thickness. Selective reflection wavelengths, λ_R, less than 3 μm were measured on the spectrophotometer. Helical pitch lengths, p, corresponding to a longer λ_R were measured from the Grandjean-Cano steps formed in a wedge. The center wavelength of the selective reflection band was then calculated with the well-known equation, $\lambda_R = p\bar{n}$, using the measured average refractive index, $\bar{n}$. An Abbé refractometer (Bellingham and Stanley Model 60/HR) with a sodium lamp (589 nm) was used to measure the extraordinary and ordinary refractive indices, $\bar{n}_{e,ch}$ and $\bar{n}_{o,ch}$, of the III-0.07 film. These values were used to calculate $\bar{n}$ and optical birefringence, Δn, of the quasinematic layer via $\Delta n = \{2n_{o,ch}^2 - n_{e,ch}^2\}^{1/2} - n_{e,ch}$.[19] Because Δn of VI-0.07 could not be measured by refractometry near the emission wavelength of 390 nm, that of VI-0.00 was measured by a phase-difference technique over a broad wavelength range.[20] This measurement was performed on the spectrophotometer by placing the nematic film, VI-0.00, between parallel UV linear polarizers with the nematic director oriented at 45° to the fast axis of each polarizer. The results are presented in Figure 3, showing a wavelength dispersion of Δn, with a value of 0.20 at 589 nm, in agreement with the refractometric data: n_e = 1.698 and n_o = 1.495.

Anisotropic Absorption and Photoluminescence. Nematic films 1.0 μm thick were prepared for the measurement of UV dichroism (Perkin-Elmer Lambda 9), $A_{\parallel}$ and $A_{\perp}$, the absorbance measured parallel and perpendicular, respectively, to the nematic director. The average absorbance was then calculated withm $A = (A_{\parallel} + 2A_{\perp})/3$, and the absorption coefficient, A/τ, was determined, where τ denotes film thickness. In situations where $A_{\parallel}$ was too high to be accurately measured, the absorbance at 45°, $A_{\pi/4}$, was measured instead,

which together with $A_\perp$ was then used to calculate A/τ. The local absorption by quasinematic layers comprising the chiral-nematic film is characterized by the resultant A/τ. Steady-state LPPL and CPPL measurements were made on a spectrofluorometer (Perkin-Elmer MPF-66). Because measurements of polarization are affected by the angle of excitation or emission, polarization control was implemented with optical elements for polarized PL experiments as shown in Figure 2 of ref 21. Background radiation from the excitation source was filtered using a band-pass filter (UG 11, Schott Glass Technologies) or color filter (BG-12, Schott Glass Technologies), depending on the emission and excitation wavelengths. To minimize optical loss due to reflection, an index matching fluid with $\bar{n} = 1.500$ (Cargille Laboratories Inc.) was placed between the sample device and the band-pass filter. For the characterization of polarized PL of III-0.00, a 370 nm UV lamp (UVP, Inc.) with a full width at half-maximum of 15 nm was used without the grating system. Because of the insufficient absorption at 370 nm by films of VI-0.00, VI-0.07, and VII, the xenon light source with grating was used for excitation at 350 nm. This excitation source was determined to have a polarization ratio of 1.5.

III. Interpretation of LPPL and CPPL Data

Conditions were established for isolating PL attributable to the conjugated backbone. In the interpretation of LPPL and CPPL data as presently pursued, it was assumed that both the absorption and emission transition dipole moments are parallel to the conjugated backbone. A chiral-nematic film consists of a stack of helically placed quasinematic layers characterized by S_{ab}, the order parameter governing anisotropic absorption, and S_{em} (or $\langle P_2 \rangle$) and $\langle P_4 \rangle$, the second- and fourth-rank order parameters governing anisotropic emission. In principle, these three order parameters can be estimated with the corresponding nematic film processed under the same condition as the chiral-nematic film. However, difficulty was encountered in situations where UV−vis absorption of the conjugated backbone overlaps with that of the pendant group [e.g., in the poly(*p*-phenylene) series]. Although IR dichroism of the C≡N stretching band at 2215 cm^{-1} is unique to the pendant cyanobiphenyl group, the resultant S_{ab} may not be a valid measure of the order assumed by the conjugated backbone. Therefore, LPPL was characterized for nematic films for the determination of S_{em} and $\langle P_4 \rangle$ within the framework of an established theory[22] with a further assumption that $S_{ab} = S_{em} = S$. The degree of CPPL is quantified by $g_e \equiv 2(I_L - I_R)/(I_L + I_R)$, in which I_L and I_R are the left- and right-handed (LH and RH) circularly polarized intensity, respectively. For pure single-handed circular polarization, g_e assumes a value of ± 2. According to a recent theory of CPPL,[23] g_e is a function of A/τ, $\bar{n}$, and Δn, all independently evaluated with nematic films. An experimentally measured g_e value was then utilized to perform a two-parameter fit to S and $\langle P_4 \rangle$. This was accomplished by initially setting $\langle P_4 \rangle$ to zero and finding S via minimization of the error between the calculated and the observed g_e. The fitted S was fed back into the theory to refine $\langle P_4 \rangle$, and the updated $\langle P_4 \rangle$ served to refine S. The numerical procedure was repeated until both S and $\langle P_4 \rangle$ reached their respective convergent values.

IV. Results and Discussion

The properties of monomers and polymers synthesized for the present study are summarized in Table 1. A previously reported nematic glass-forming liquid crystal, depicted as VII in Figure 1, is included for assessing the PL intensity of the cyanobiphenyl group relative to that of the poly(*p*-phenylene) backbone. In all four monomers, the aromatic rings are separated from the pendants by a flexible spacer. Therefore, it is believed that statistical copolymers are more likely to form than block copolymers. This is supported by the observation that the copolymer ratio determined by NMR spectroscopy is consistent with the feed composition, indicating equal reactivity of comonomers. It is noted that Ni(0)-catalyzed polymerization produced polymers with relatively low molecular weights. However, the above-ambient T_g and good film-forming ability of the polymer products permitted us to explore polarized PL. No efforts were made in this study to control the regiochemistry of the resultant polymers or to achieve a high degree of polymerization. The reported thermal transition temperatures were based on the DSC heating scans at 20 °C/min of samples pretreated to above T_m or T_c followed by cooling at −20 °C/min to −30 °C. Note that all the monomers and polymers are capable of glass formation and that between T_g and T_c all the polymers possess either a nematic or a cholesteric mesophase, identified as threaded textures or oily streaks, respectively. With naturally occurring (−)-cholesterol as the chiral building block, III-0.07, -0.16, -0.29 and VI-0.07 were found to present left-handed helical structures, as expected;[24] note that the handedness of the helical structure is defined by the reflected light. Dilute solutions in methylene chloride were prepared at 10^{-5} M on the basis of monomer and repeat units for UV−vis spectrophotometric characterization. The absorption spectra are presented in Figure 4 in terms of molar extinction coefficient, ϵ. As spectra **c**, **d**, and **e** are compared to spectra **a** and **b**, it is clear that the polythiophene backbone contributes to absorption above 350 nm, where monomers I and II are transparent. Therefore, it is possible to selectively photoexcite the polythiophene backbone. A 22 μm thick film of polymer III-0.07 was prepared according to the procedures described in section II for the characterization of CPPL.

Table 1. Properties of Monomers and Mesomorphic Conjugated Polymers[a,b]

material system	$\bar{M}_n$	$\bar{M}_w$	POM and DSC Data (°C)
I	NA	NA	G −4 N 33 I
II	NA	NA	G 30 Ch 42 I
III-0.00	2,630	4,240	G 74 N 144 I
III-0.07	1,730	2,080	G 61 Ch 112 I
III-0.16	3,860	22,500	G 90 Ch 132 I
III-0.29	3,810	17,200	G 88 Ch 116 I
IV	NA	NA	G 1 N 14 I
V	NA	NA	G 9 I
VI-0.00	10,700	13,300	G 71 Ch 172 I
VI-0.07	8,360	9,450	G 59 Ch 122 I
VII	1,224	1,224	G 64 N 129 I

[a] Symbols: G, glassy; N, nematic; Ch, cholesteric; I, isotropic. Nematic and cholesteric mesophases were identified with threaded textures and oily streaks, respectively, by polarizing optical microscopy, POM. [b] Thermal transition temperatures were determined from heating scans at 20 °C/min of samples preheated to beyond T_c followed by cooling at −20 °C/min to −30 °C.

The CPPL spectra of the (III-0.07) film are presented in Figure 5, in which the results from both circularly polarized and unpolarized excitations at 370 nm are included. Note that g_e has a negative value because of the LH structure of the film, which reflects the LH component of the emitted light preferentially to the RH component. In Figure 5a, the emission intensities are

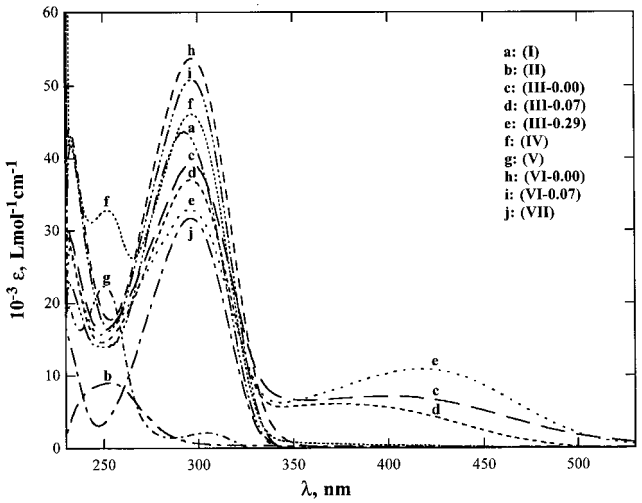

Figure 4. UV−vis spectra of all compounds in a dilute solution of methylene chloride.

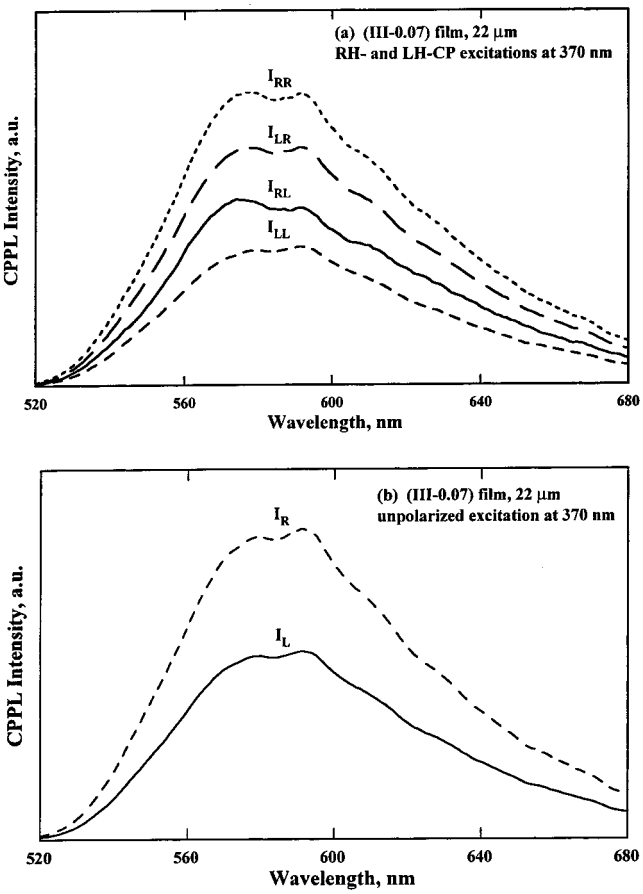

Figure 5. CPPL spectra of a 22 μm film of III-0.07: (a) right- and left-handed circularly polarized (RH- and LH-CP) excitation at 370 nm; (b) unpolarized excitation at 370 nm.

specified with two subscripts: the first indicating the handedness of excitation, and the second, that of emission. The calculated $g_{e,L}$ and $g_{e,R}$ for the LH and RH excitation remain reasonably constant at -0.46 ± 0.02 and -0.53 ± 0.02, respectively, in the spectral region from 550 to 650 nm. On the basis of CPPL theory that we have constructed,[23] the observed $g_{e,L}$ and $g_{e,R}$ values were interpreted using the following independently determined parameters: $\Delta n = 0.22$ and $\bar{n} = 1.61$, at 589 nm (i.e., near the center of the emission peak), $p = 5.00$ μm, and the absorption coefficient, $A/\tau = 16\,500$ cm^{-1} at 370 nm. It is remarked in passing that a total of four pitches exist in a 22 μm film with a pitch length of 5.00 μm. An agreement between the theory and experiment was secured with order parameters assuming the following values: $S = 0.44$ and $\langle P_4 \rangle = -0.14$. It should be noted that for $S \leq 0.60$, $\langle P_4 \rangle$ can be negative due to repulsive forces or other dipole−dipole interactions.[25] As shown in Figure 5b, the CPPL spectra with an unpolarized excitation at 370 nm resulted in a $g_e = -0.49 \pm 0.01$. With the same set of parameters, $S = 0.39$ and $\langle P_4 \rangle = -0.11$ emerged from the fit to the CPPL theory in which the unpolarized excitation was represented by the sum of equally weighted LH and RH components with a random phase relationship between the two.[26]

As shown in Figure 4 for the UV−vis absorption of monomers IV and V and polymers VI-0.00 and VI-0.07 in dilute solution, the poly(*p*-phenylene) backbone does not have a distinct absorption peak, unlike the polythiophene series. At the absorption maximum of 300 nm, the pendant cyanobiphenyl group has an extinction coefficient comparable to that of the *p*-phenylene unit comprising the conjugated backbone. However, an effort was made to isolate PL of the poly(*p*-phenylene) backbone for the interpretation of experimental data. With the assumption that the number density of the repeat units in the VI-0.00 film is equal to that in VII, it was estimated that $A/\tau = 6510$ and 4690 cm^{-1} at 350 nm for the conjugated backbone and the pendant cyanobiphenyl group, respectively. Without polarization control or analysis of the excitation or emission beam, PL spectra were collected in a front-face arrangement for a horizontal and a vertical orientation of the nematic director; the average of these two spectra is reported in Figure 6a for the two nematic films. It is shown that the emission intensity of VI-0.00 at the emission maximum (400 nm) is 1 order magnitude stronger than that of VII, suggesting a much higher PL quantum yield for the conjugated backbone than the pendant cyanobiphenyl group. This comparison is legitimized by the observation to be made below that these two films possess comparable order parameters. Therefore, to a very good approximation, PL of both the VI-0.00 and the VI-0.07 films could be treated as originating from the poly(*p*-phenylene) backbone.

Linearly polarized PL of the (VI-0.00) film was further characterized for the determination of order attributable to the conjugated backbone. As shown in Figure 6b, the VI-0.00 film with an excitation at 350 nm, linearly polarized along the nematic director, produced linearly polarized PL. A fit to the LPPL theory resulted in $S = 0.31$ and $\langle P_4 \rangle = -0.29$. A similar analysis of the VII film led to $S = 0.38$ and $<P_4> = -0.20$, which characterize the order attributable to the cyanobiphenyl group. A 22 μm thick film was prepared with polymer VI-0.07, and its selective reflection spectrum is shown in Figure 7, indicating a $\lambda_R = 2.14$ μm. Relevant optical properties were determined as follows: $\Delta n = 0.25$ and $\bar{n} = 1.63$, both at 410 nm (see Figure 3) where maximum CPPL intensities occur, and $A/\tau = 6510$ cm^{-1} at 350 nm for the conjugated backbone. With $p = \lambda_R/\bar{n} = 1.32$ μm, the 22 μm thick VI-0.07 film consists of 17 pitches. The CPPL spectra shown in Figure 7 yielded $g_{e,L} = -0.20$ and $g_{e,R} = -0.31$, which produced $S = 0.26$ and $\langle P_4 \rangle = -0.16$ in the context of the CPPL theory. From a practical perspective, the presently reported g_e values are 2 orders of magnitude higher than those observed

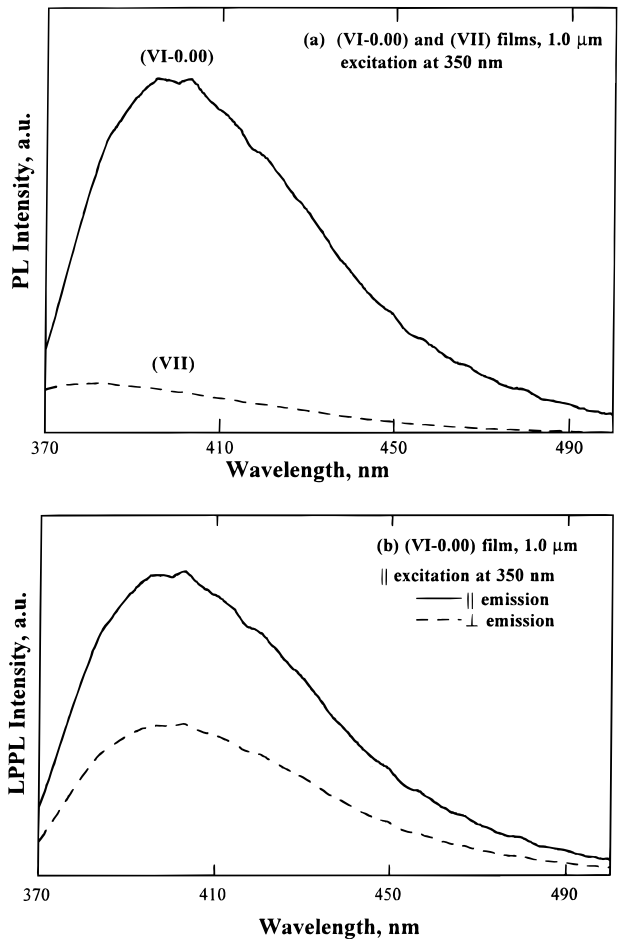

Figure 6. (a) Relative PL intensities of 1.0 μm films of VI-0.00 and VII with excitation at 350 nm. (b) LPPL spectra of a 1.0 μm film of VI-0.00 with excitation at 350 nm parallel to nematic director.

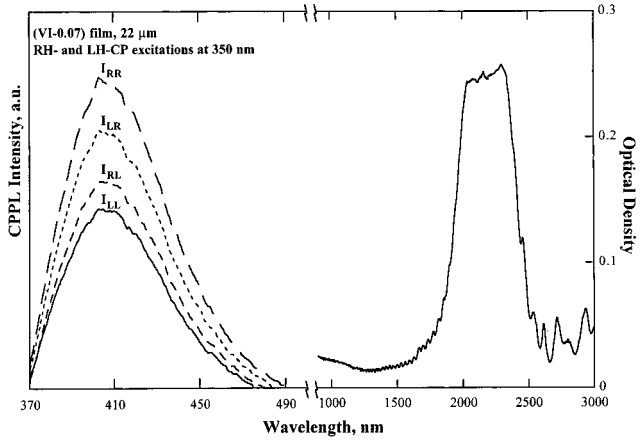

Figure 7. Selective wavelength reflection and CPPL spectra of a 22 μm film of VI-0.07 with RH-CP and LH-CP excitation at 350 nm.

for a polythiophene backbone carrying chiral pendants.[15] It is evident that chirality due to the self-assembly of π-conjugated segments, as mediated by the cholesteric mesomorphism, is superior to chirality of individual π-conjugated segments imparted by pendant groups in the realization of CPPL.

V. Summary

Novel thermotropic nematic and left-handed chiral-nematic polythiophene and poly(*p*-phenylene) derivatives were synthesized and characterized using cyanobiphenyl and (−)-cholesterol as the nematogenic and chiral pendant group, respectively. With T_g ranging from 59 to 90 °C and T_c from 112 and 172 °C, these polymers were readily processed into uniaxially and helically aligned solid films for polarized PL studies. In the thiophene series, UV−vis spectra in dilute solution revealed absorption peaks between 350 and 500 nm that were absent in monomers and hence attributable to the conjugated backbone. Unpolarized excitation at 370 nm allowed PL of the aligned polythiophene backbones to be selectively observed between 550 and 650 nm. A chiral-nematic glassy film with a $p = 5.00$ μm produced a g_e of −0.49, which is significant considering the facts that emission occurs in a loosely pitched film and that $|g_e| = 2$ for pure, single-handed circularly polarized PL. In the *p*-phenylene series, no absorption peaks were exclusively attributable to the conjugated backbone. In fact, the pendant cyanobiphenyl group and the poly(*p*-phenylene) backbone were found to have comparable absorption coefficients at 300 nm. However, it was found that with excitation at 350 nm, the *p*-phenylene unit in the conjugated backbone is more luminescent than the cyanobiphenyl pendant by 1 order of magnitude. Therefore, PL observed with solid films of poly(*p*-phenylene) derivatives was treated as originating in the conjugated backbone. A chiral-nematic poly(*p*-phenylene) derivative was processed into a film with $p = 1.31$ μm, resulting in $g_e = -0.31$ and −0.20 with a RH and LH circularly polarized excitation at 350 nm, respectively. As input data for the theories governing polarized PL, absorption coefficient, average refractive index, and optical birefringence were independently determined. The experimentally observed linearly and circularly polarized PL of both the polythiophene and poly(*p*-phenylene) derivatives were found to be in good agreement with existing theories with *S* assuming a value between 0.26 and 0.44.

Acknowledgment. We express our gratitude for helpful discussions with and technical assistance of Drs. S. D. Jacobs and A. W. Schmid, and Mr. K. L. Marshall of the Laboratory for Laser Energetics, University of Rochester. This work was supported by the National Science Foundation under Grants CHE-9120001 and CTS-9500737. Additional support was provided by the U.S. Department of Energy Office of Inertial Confinement Fusion under Cooperative Agreement No. DE-FC03-92SF19460, the University of Rochester, and the New York State Energy Research and Development Authority. The support of DOE does not constitute an endorsement by DOE of the views expressed in this article. D.U.K. was supported in part by the South Korean Science Foundation.

References and Notes

(1) Schadt, M.; Fünfschilling, J. *Jpn. J. Appl. Phys.* **1990**, *29*, 1974.
(2) Adam, D.; Schuhmacher, P.; Simmerer, J.; Häussling, L.; Siemensmeyer, K.; Etzbach, K. H.; Ringsdorf, H.; Haarrer, D., *Nature* **1994**, *371*, 141.
(3) Katz, H. E. *J. Mater. Chem.* **1997**, *7*, 369.
(4) Burroughes, J. H.; Bradley, D. D. C.; Brown, A. R.; Marks, R. N.; Mackay, K.; Friend, R. H.; Burn, P. L.; Kraft, A.; Holmes, A. B. *Nature* **1990**, *347*, 539.
(5) Gustafsson, G.; Cao, Y.; Treacy, G. M.; Klavetter, F.; Colaneri, N.; Heeger, A. J. *Nature* **1992**, *357*, 477.
(6) Vicentini, F.; Barrouillet, J.; Laversanne, R.; Mauzac, M.; Bibonne, F.; Parneix, J. P. *Liq. Cryst.* **1995**, *19*, 235.

(7) Lüssem, G.; Festag, R.; Greiner, A.; Schmidt, C.; Unterlechner, C.; Heitz, W.; Wendorff, J. H.; Hopmeier, M.; Feldmann, J. *Adv. Mater.* **1995**, *7*, 923.
(8) Yoshino, K.; Yin, X. H.; Morita, S.; Nakazono, M.; Kawai, T.; Ozaki, M.; Jin, S. H.; Choi, S. K. *Jpn. J. Appl. Phys.* **1993**, *32*, L1673.
(9) Dirix, Y.; Tervoort, T. A.; Bastiaansen, C. *Macromolecules* **1995**, *28*, 486.
(10) Good, R. H., Jr.; Karali, A. *J. Opt. Soc. Am. A* **1994**, *11*, 2145.
(11) Hagler, T. W.; Pakbaz, K.; Voss, K. F.; Heeger, A. J. *Phys. Rev. B* **1991**, *44*, 8652.
(12) Weder, C.; Sarwa, C.; Bastiaansen, C,; Smith, P. *Adv. Mater.* **1997**, *9*, 1035.
(13) Cimrová, V.; Remmers, M.; Neher, D.; Wegner, G. *Adv. Mater.* **1996**, *8*, 146.
(14) Sariciftci, N. S.; Lemmer, U.; Vacar, D.; Heeger, A. J.; Janssen, R. A. J. *Adv. Mater.* **1996**, *8*, 651.
(15) Langeveld-Voss, B. M. W.; Janssen, R. A. J.; Christiaans, M. P. T.; Meskers, S. C. J.; Dekkers, H. P. J. M.; Meijer, E. W. *J. Am. Chem. Soc.* **1996**, *118*, 4908.
(16) Shi, H.; Conger, B. M.; Katsis, D.; Chen, S. H. *Liq. Cryst.* **1998**, *24*, 163.
(17) Chen, S. H.; Mastrangelo, J. C.; Conger, B. M.; Kende, A. S.; Marshall, K. L. *Macromolecules* **1998**, *31*, 3391.
(18) Chen, S. H.; Mastrangelo, J. C.; Blanton, T. N.; Bashir-Hashemi, A. *Liq. Cryst.* **1996**, *21*, 683.
(19) Lee, J. C.; Jacobs, S. D. *J. Appl. Phys.* **1990**, *68*, 6523.
(20) Wu, S. T.; Efron, U.; Hess, L. D. *Appl. Opt.* **1984**, *23*, 3911.
(21) Conger B. M.; Mastrangelo, J. C.; Chen, S. H. *Macromolecules* **1997**, *30*, 4049.
(22) Wolarz, E.; Bauman, D. *Mol. Cryst. Liq. Cryst.* **1991**, *197*, 1.
(23) Shi, H.; Conger, B. M.; Katsis, D.; Chen, S. H. *Liq. Cryst.* **1998**, *24*, 163.
(24) Tsai, M. L.; Chen, S. H. *Macromolecules* **1990**, *23*, 1908.
(25) Jen, S.; Clark, N. A.; Pershan, P. S.; Priestley, E. B. *Phys. Rev. Lett.* **1973**, *31*, 1552.
(26) Saleh, B. A.; Teich, M. R. *Fundamentals of Photonics*; John Wiley & Sons: New York, 1991; p 378.

MA980945P